Characterization and Manipulation of Exposed Ge Nanocrystals

I.D. Sharp[a,b], Q. Xu[a,b], C.Y. Liao[a,b], D.O. Yi[a,c], J.W. Ager III[a], J.W. Beeman[a], K.M. Yu[a], D.N. Zakharov[a], Z. Liliental-Weber[a], D. C. Chrzan[a,b], E.E. Haller[a,b]
[a]Materials Science Division, Lawrence Berkeley National Laboratory, Berkeley, CA 94720
[b]Department of Materials Science and Engineering, University of California, Berkeley, CA 94720
[c]Applied Science and Technology Graduate Group, University of California, Berkeley, Berkeley, CA 94720

ABSTRACT

Isotopically pure ^{70}Ge and ^{74}Ge nanocrystals embedded in SiO_2 thin films on Si substrates have been fabricated through ion implantation and thermal annealing. Nanocrystals were subsequently exposed using a hydrofluoric acid etching procedure to selectively remove the oxide matrix while retaining up to 69% of the implanted Ge. Comparison of transmission electron micrographs (TEM) of as-grown crystals to atomic force microscope (AFM) data of exposed crystals reveals that the nanocrystal size distribution is very nearly preserved during etching. Therefore, this process provides a new means to use AFM for rapid and straightforward determination of size distributions of nanocrystals formed in a silica matrix. Once exposed, nanocrystals may be transferred to a variety of substrates, such as conducting metal films and optically transparent insulators for further characterization.

INTRODUCTION

With the exception of those synthesized by chemical means, semiconductor nanocrystals are typically embedded in a host matrix, usually SiO_2. While this may be desirable for the fabrication of conventional solid-state devices [1], it is not conducive to comprehensive surface and electronic characterization or manipulation. Therefore, it is desirable to develop a method to selectively remove the matrix and obtain free-standing nanocrystals. Such a process will provide a means to directly and individually contact nanocrystals, thereby significantly increasing the number of available characterization techniques and providing a means for nanomanipulation [2].

It is often desirable to transfer nanocrystals to other substrates for further characterization; Lacy carbon grids allow for rapid characterization using transmission electron microscopy (TEM), extremely flat and conducting substrates are required for scanning tunneling microscopy (STM), and optically transparent substrates are required for optical absorption measurements. Once liberated, nanocrystals may be transferred to these, or other, substrates.

Two methods are currently available for determining the size distributions of nanocrystals: TEM and Raman spectroscopy. TEM requires painstaking sample preparation and has a very limited sampling of nanocrystal sizes. Fitting Raman spectra using phonon confinement models is relatively inaccurate owing to the dependence of the weighting function on the specific form of the confining function [3] and is typically only

used to obtain a rough estimate of the average nanocrystal size. Using the liberation process, it will be possible to rapidly determine nanocrystal size distributions using an atomic force microscope (AFM). This technique has a number of advantages. AFMs are typically more accessible than TEMs, no arduous sample preparation is required, and there is virtually no limit to the sampling size. This last point is particularly advantageous, as it provides enhanced statistical reliability over other existing techniques.

EXPERIMENTAL DETAILS

Ge nanocrystals were fabricated by ion implantation of ^{70}Ge or ^{74}Ge ions into a 500 nm thick SiO_2 thin film on a Si substrate followed by thermal annealing at 900 °C for 1 hour. Multi-energy implantation at 50 keV (1×10^{16} cm^{-2}), 80 keV (1.2×10^{16} cm^{-2}), and 120 keV (2×10^{16} cm^{-2}) was used to obtain a more constant Ge concentration in the growth region [4]. Thermal annealing was performed in an ampoule under 120 mTorr Ar to ensure good thermal coupling to the surrounding environment. Annealing was terminated by quenching under cold running water.

Selective removal of the SiO_2 matrix was achieved via etching in an aqueous solution of 1:1 49% HF:H_2O. TEM, RBS, and Raman spectroscopy were used to compare as-grown nanocrystals embedded in the oxide matrix to free-standing nanocrystals. To reduce the density of free-standing nanocrystals on the surface, samples were immersed in methanol and ultrasonically cleaned for times between 15 minutes and 1 hour. After sonication, AFM was performed to determine nanocrystal size distributions. Nanocrystals were transferred between surfaces by immersing clean substrates in the nanocrystal-containing methanol solution and drying under flowing nitrogen.

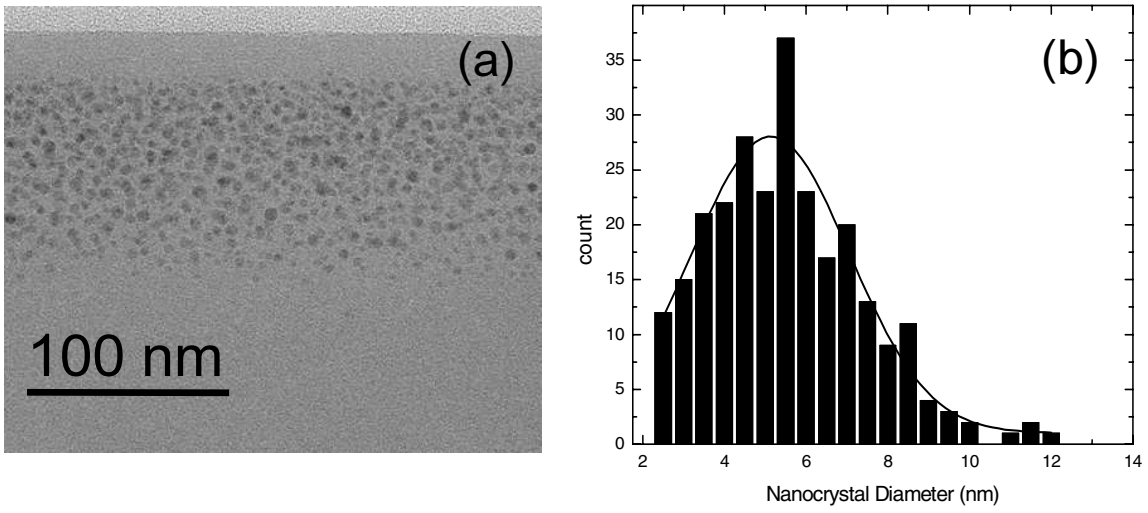

Fig. 1: Transmission electron micrograph of Ge nanocrystals embedded in SiO_2 (a) and the corresponding size distribution determined by analysis of TEM images (b). The distribution is fit with a Gaussian function and gives an average nanocrystal diameter of 5.1 nm with a distribution FWHM of 3.9 nm.

RESULTS AND DISCUSSION

TEM images of as-grown samples reveal a narrow nanocrystal band in the near surface region of the oxide film, as shown in Fig. 1(a). Image analysis of TEM micrographs yields the nanocrystal size distribution presented in Fig. 1(b). A Gaussian fit to the size distribution gives an average nanocrystal diameter of 5.1 nm with a distribution full width at half maximum (FWHM) of 3.9 nm.

After selective removal of the oxide matrix, Ge nanocrystals are retained on the surface. Comparison of RBS spectra obtained before and after etching reveals that 69% of the originally implanted Ge accumulates on the surface after complete removal of the SiO_2. Attractive van der Waals forces are likely responsible for this buildup of nanocrystals. The theoretical basis of these forces is well-established [5,6] and additional experiments are underway to determine their magnitudes in the current Ge nanocrystal system.

Fig. 2 shows an AFM image of Ge nanocrystals on the Si substrate obtained after etching. A loosely packed layer of nanocrystals is observed and there is no evidence of significant agglomeration to form larger particles. However, to obtain nanocrystal size distributions using AFM, it is necessary to image isolated nanocrystals. Ultrasonic treatment of etched samples significantly reduces the density of nanocrystals on the surface. Fig. 3(a) shows an AFM image obtained after 15 minutes of sonication. Isolated nanocrystals are observed. Since in-plane size data are dominated by the probe-tip radius, the heights of nanocrystals on the Si substrate are used to determine nanocrystal sizes. Fig. 3(b) shows the size distribution obtained in this manner along with a Gaussian fit to the data. The average crystal size using this technique is 5.1 nm with a distribution FWHM of 3.4 nm, in excellent agreement with TEM results. Thus, the nanocrystal size distribution is not significantly affected by HF etching or ultrasonic cleaning. As a result, AFM may be used for rapid determination of size distributions. A number of experiments will be performed in the future to correlate growth conditions to the size distributions of nanocrystals. Previously, this was not possible because of the time consuming sample preparation required for TEM analysis. The size distribution is also preserved after nanocrystals are transferred to other substrates by immersion in the nanocrystal-containing methanol solution.

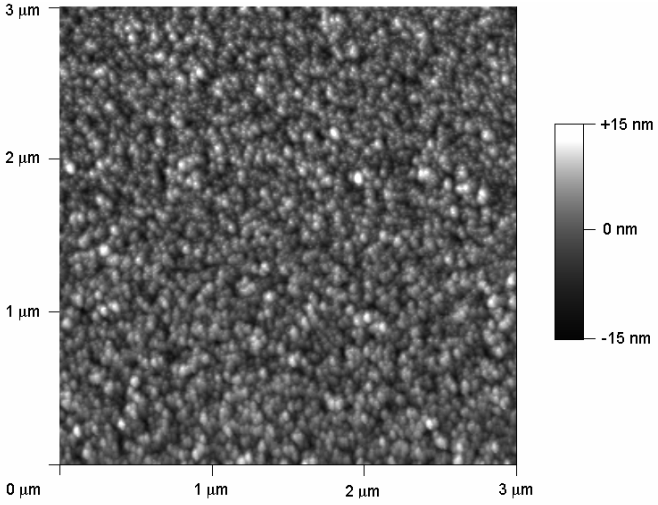

Fig. 2: Atomic force microscope image of free-standing Ge nanocrystals on a Si substrate after selective removal of the oxide matrix. Nanocrystals are loosely packed on the surface and there is no evidence of agglomeration of the crystals. Size distribution data may not be obtained from images such as this due to the high particle density.

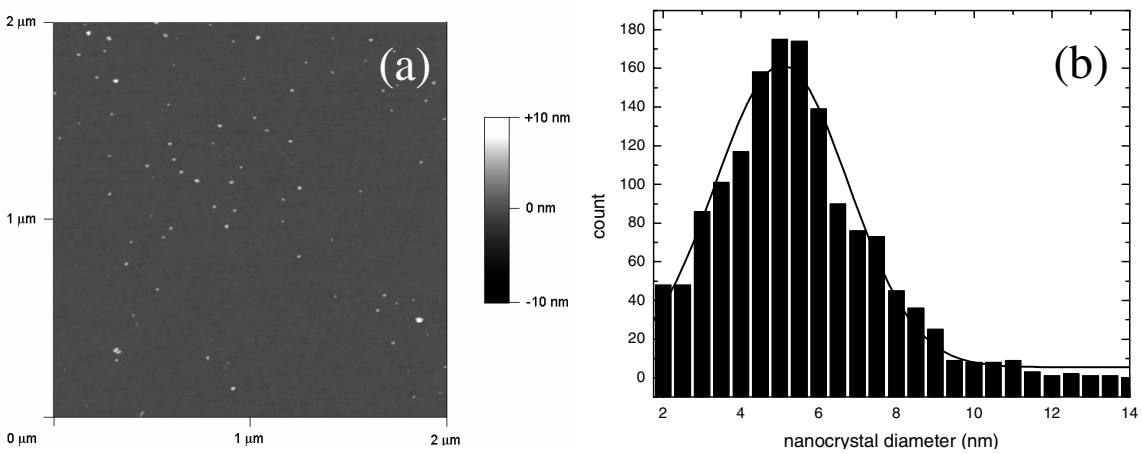

Fig. 3: Atomic force microscope image of isolated free-standing Ge nanocrystals on a Si substrate after chemically selective removal of the oxide matrix and ultrasonic treatment in methanol for 15 minutes (a). Nanocrystal size distribution obtained from height data of multiple AFM images (b). The distribution is fit with a Gaussian function which gives an average nanocrystal size of 5.1 nm and a distribution FWHM

Raman spectra of as-grown nanocrystals exhibit the expected asymmetric line broadening consistent with the breakdown of selection rules which lead to non-zone center optical phonon transitions ($\vec{k} \neq 0$) [7]. However, comparison of Raman spectra from as-grown ^{74}Ge nanocrystals [Fig. 4(a)] to isotopically enriched bulk ^{74}Ge samples [Fig. 4(c)] reveals a blue-shift that is not predicted for confined phonons. Such a shift is consistent with the presence of significant compressive stress [8]. It is shown elsewhere that this stress may be controllably relieved via post-growth thermal annealing below the growth temperature [9].

Fig. 4(b) shows a Raman spectrum from free-standing nanocrystals obtained immediately after HF etching. Asymmetric line broadening is again observed. However, the peak position is red-shifted in relation to the bulk reference sample. This shift is consistent with the predictions of phonon confinement models and indicates that the

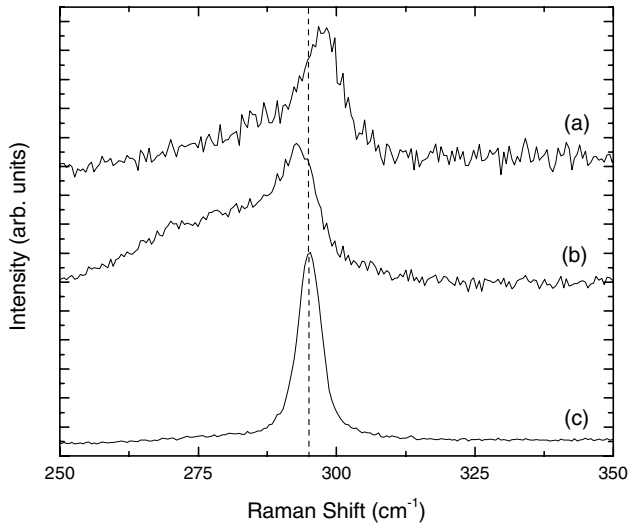

Fig. 4: Raman spectra of as-grown nanocrystals (a), free-standing nanocrystals after selective removal of the oxide matrix (b), and an isotopically enriched bulk sample (c). The as-grown spectrum is blue shifted in relation to all other spectra, indicating the presence of compressive stress. After etching, an additional low energy peak emerges which is indicative of surface vibrational modes.

matrix is responsible for the stress exerted on as-grown nanocrystals. After etching, a low energy tail emerges in the Ge nanocrystal Raman spectrum, as demonstrated in Fig 4(b). Since the nanocrystal size distribution is not affected by the etching procedure, enhanced confinement of phonons is not responsible for the observed lineshape. Subtraction of the as-grown spectrum from the etched spectrum, after shifting the as-grown peak such that the right shoulders of the two spectra overlap, yields an amorphous-like Raman peak centered at 276 cm^{-1}. This has been observed previously and likely arises from low energy surface vibrational modes [10,11]. When the nanocrystals are embedded and stressed, these modes are suppressed through interactions with the matrix. However, upon liberation, the surface atoms are less tightly bound than interior atoms. These results are consistent with recent theoretical calculations been used to determine surface vibrational modes of Ge nanocrystals [12]. It is not yet clear if the wide nanocrystal size distribution will preclude observation of other surface phonon modes.

No significant change of the Raman spectrum of etched nanocrystals is observed after extended exposure to ambient atmospheric conditions. Formation of a bulk-like native oxide layer would consume the majority of nanocrystals and lead to a significant change of the Raman signal over time. It has been shown previously that nanostructures may have self-limiting native oxide thicknesses arising from the very small radius of curvature of their surfaces [13]. Some oxidation of the Ge nanocrystals is expected but the thickness is significantly reduced from the bulk case, which is consistent with the self-limiting native oxide formation mechanism in nanostructures.

Fig. 5 shows AFM images of Ge nanocrystals that have been transferred to a Si surface by immersion in the methanol solution after ultrasonic cleaning of an etched sample. Fig. 5(a) shows that nanocrystals may be moved along the surface using the AFM probe. When the same region is imaged a second time with lighter tapping, the nanocrystals remain stationary in their new positions. Currently, direct manipulation of the Ge nanocrystals in not controllable, which is the case shown in Fig. 5. However,

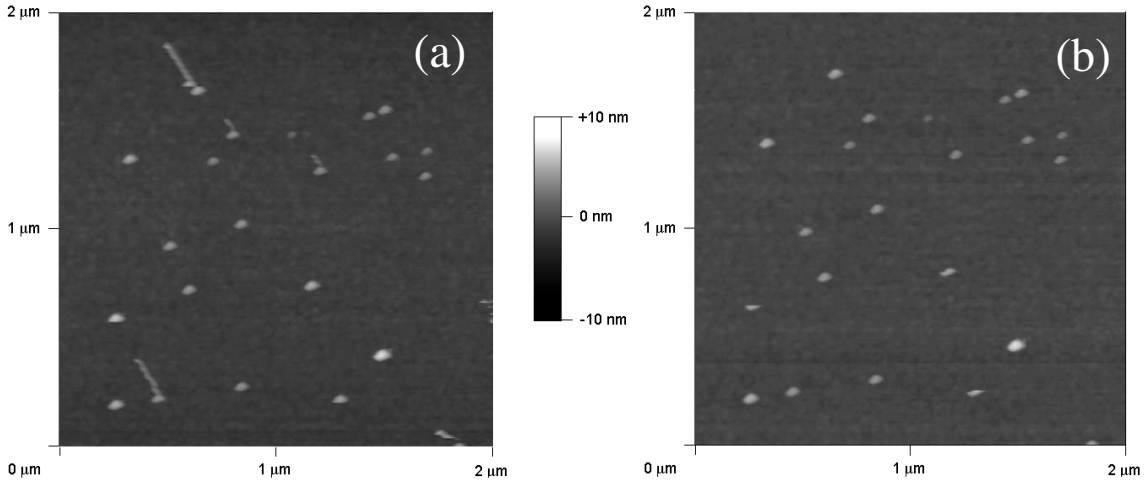

Fig. 5: AFM images of nanocrystals after transfer to a silicon surface. Nanocrystals are "pushed" along the surface by the AFM probe tip (a). The scan direction is from the top of the image downward. Nanocrystals are stationary when the same region is scanned with lighter tapping force. The positions of nanocrystals in (b) correspond to the final positions of nanocrystals from (a) after manipulation.

these results illustrate that nanocrystals are mobile on the surface and vdW interaction forces are not sufficient to prevent nanomanipulation. Experiments are underway to controllably manipulate nanocrystals in order to form two- and three-dimensional arrays.

CONCLUSION

A process to expose the surfaces of ion beam synthesized nanocrystals embedded in SiO_2 thin films has been developed. Selective removal of the oxide matrix is achieved by HF etching. Nanocrystals accumulate on the surface during the etching process and their size distribution is not significantly affected during processing. Nanocrystal size distributions obtained using AFM are in excellent agreement with those obtained via TEM. Raman spectra indicate that as-grown nanocrystals experience large compressive stresses. Removal of the matrix removes the source of stress and relaxed free-standing nanocrystals are observed. Free-standing nanocrystals, which are stable in ambient atmospheric conditions, exhibit additional vibrational modes arising from their exposed surface atoms. Nanocrystals may be transferred between surfaces, thus increasing the number of available techniques for characterization of nanocrystals. Preliminary results indicate that direct contact manipulation of free-standing Ge nanocrystals to form ordered structures will be possible.

ACKNOWLEDGEMENTS

I.D.S. acknowledges support from the Intel Robert N. Noyce fellowship. D.O.Y. acknowledges support from the U.C. Berkeley and Luce Foundation Fellowships. Q.X. acknowledges support through a U.C. Berkeley Fellowship. D.C.C. and E.E.H. acknowledge support by the Miller Institute for Basic Research in Science. This work is supported in part by the Director, Office of Science, Office of Basic Energy Sciences, Division of Materials Science and Engineering, of the U.S. Department of Energy under contract No. DE-AC03-76F00098 and in part by U.S. NSF Grant Nos. DMR-0109844 and EEC-0085569.

REFERENCES

[1] S. Tiwari, *et al.*, Appl. Phys. Lett. **69**, 1232 (1996).
[2] S. Decossas, *et al.*, Nanotechnology **14**, 1272 (2003).
[3] I. H. Campbell and P. M. Fauchet, Solid State Commun. **58**, 739 (1986).
[4] M. Yamamoto, *et al.*, Thin Solid Films **369**, 100 (2000).
[5] H. C. Hamaker, Physica **4**, 1058 (1937).
[6] J. N. Israelachvili, *Intermolecular and Surface Forces*. (Academic Press, London, 1985).
[7] H. Richter, Z. P. Wang and B. Ley, Solid State Commun. **39**, 625 (1981).
[8] F. Cerdeira, *et al.*, Phys. Rev. B **5**, 580 (1972).
[9] D. O. Yi, *et al.*, MRS Spring Meeting, Symposium P, (San Francisco, 2004).
[10] M. Fujii, S. Hayashi and K. Yamamoto, Jpn. J. Appl. Phys. **30**, 687 (1991).
[11] A. G. Rolo, *et al.*, Thin Solid Films **336**, 58 (1998).
[12] W. Cheng, S.-F. Ren and P. Y. Yu, Phys. Rev. B **68**, 193309 (2003).
[13] H. I. Liu, *et al.*, Appl. Phys. Lett. **64**, 1383 (1994).